

ARTICLE OPEN



Avoidable heat-related mortality in China during the 21st century

Guwei Zhang^{1,2,3,4}, Zhaobin Sun^{2,5}, Ling Han⁵, Vedaste Iyakaremye⁶, Zhiqi Xu^{1,3}, Shiguang Miao^{1,3} and Shilu Tong^{7,8,9,10}✉

Using non-accidental mortality records from 195 sites and 11 model simulations from the Coupled Model Intercomparison Project phase 6, we assessed future avoidable heat-related deaths associated with emission mitigation after accounting for population changes in China. Without human-induced climate change in the 21st century, China's heat-related mortality would drop by 48–72% (95% confidence interval (CI): 40–76%), especially at high latitudes and altitudes (up to 80%). Nationally, 15,576–87,612 (95% CI: 6605–106,736) heat-related deaths per year would potentially be avoided by reducing emissions. For most of China, temperature changes dominate the variation in heat-related deaths, while in Central and South China, population changes will have a greater influence. These not only reinforce the necessity of mitigating emissions but also suggest that adjusting population structure and spatial distribution could be applied in some areas to minimize warming impacts on public health. Notably, given that abatement will hardly bring immediate success within the next twenty years, more healthcare infrastructures are urgently needed to manage potential growing heat risks. Particularly in Northwest and South China, where future heat-related deaths would still be 110–140% of current levels (1995–2014) even without anthropogenic warming. We also found that without historical human-induced emissions, China's low level of technology (medical and economic) might increase current heat-related mortality by 57%, even though warming could be mitigated. Consequently, we believe that mitigating climate change risks also requires consideration of the economic/medical losses from lowering emissions.

npj Climate and Atmospheric Science (2023)6:81 ; <https://doi.org/10.1038/s41612-023-00404-4>

INTRODUCTION

Rising temperatures driven by increased carbon emissions have become one of the most dangerous climate risks to public health¹. Notably, global greenhouse gas emissions have peaked in human history in the last decade (2011–2020), and extreme heat events occur frequently around the world^{2,3}. Hot weather can raise the body's core temperature and heartbeat rate, resulting in heat stroke, respiratory and cardiovascular diseases, and even death⁴. For example, the 1995 Chicago heatwave caused 739 deaths⁵. The 2003 extreme high-temperature event in Europe killed at least 70,000 people⁶. Over 50,000 Russian residents died from the 2010 heatwave⁷. Nearly 600 people died in North America from persistent hot weather in 2021⁸. As climate change proceeds, thermal risks (e.g., heat-related mortality) in many regions of the world will be shocking, particularly in populated metropolitan areas^{9–11}. Considering the present critical situation, substantially reducing carbon emissions to mitigate negative impacts on public health is imperative^{2,3}.

In the latest Assessment Reports, the Intergovernmental Panel on Climate Change (IPCC) considered comprehensive factors to quantify the relationship between climate change and socio-economic development¹², proposing new emissions scenarios combining shared socioeconomic pathways (SSPs) with the climate representative concentration pathways (RCPs)^{13,14}. Under these new scenarios, the Coupled Model Intercomparison Project

phase 6 (CMIP6) has provided the latest climate projections¹⁵. Many studies have applied the CMIP6 datasets to project climate patterns worldwide^{11,16–19}. China's intervention to mitigate and adapt to climate change is crucial and will provide significant health benefits to about 1.4 billion people, and incorporating these strategies into detailed pathways to achieve carbon neutrality commitments will ensure improved human health and well-being^{20,21}. Some researchers combined demographic projections and mortality records to assess the future health risks associated with exposure to heat conditions in China^{9,10,19,22,23}. However, most previous efforts have paid limited attention to quantifying how much heat-related risk can be avoided by maximizing emission reductions^{24,25}. These projections are not sufficient to effectively plan the infrastructure needed.

The world is now ~1.0 °C warmer than the pre-industrial era²⁶, and China, a country with a large population, is experiencing warming beyond that level²⁷. Extreme heat events across China have frequently occurred since this century, causing many deaths^{11,22,27,28}. Given the continuing population growth²⁹, coupled with rising temperatures^{30,31}, governments should build the necessary health infrastructures to cope with the expected changes and prioritize prevention efforts in the areas where influences are concentrated³². Although many studies have been carried out to assess future heat events and health risks in China^{9,11,23,33}, there still needs more work to quantify the

¹Institute of Urban Meteorology, China Meteorological Administration, 100089 Beijing, China. ²State Key Laboratory of Severe Weather, Chinese Academy of Meteorological Sciences, China Meteorological Administration, 100081 Beijing, China. ³Key Laboratory of Urban Meteorology, China Meteorological Administration, 100089 Beijing, China. ⁴KLME & CIC-FEMD, Nanjing University of Information Science & Technology, 210044 Nanjing, China. ⁵National Key Laboratory of Intelligent Tracking and Forecasting for Infectious Diseases, National Institute for Communicable Disease Control and Prevention, Chinese Center for Disease Control and Prevention, 102206 Beijing, China. ⁶Rwanda Meteorology Agency, Nyarugenge KN 96 St, Kigali, Rwanda. ⁷National Institute of Environmental Health, Chinese Center for Disease Control and Prevention, 100021 Beijing, China. ⁸School of Public Health, Institute of Environment and Population Health, Anhui Medical University, 230032 Hefei, China. ⁹Center for Global Health, Nanjing Medical University, 211166 Nanjing, China. ¹⁰School of Public Health and Social Work, Institute of Health and Biomedical Innovation, Queensland University of Technology, Brisbane 4059, Australia.

✉email: szb850804@163.com; tongshilu@nieh.chinaccd.cn

contributions of population changes and climate warming to heat-related deaths. Hence, this study aimed to examine the future avoidable heat-related mortality associated with climate change after accounting for population changes in China³⁴ and to quantify the independent contribution of future temperature and population changes to heat-related deaths. Our result will provide a comprehensive and updated projection of heat-related health risks in China, for strategic planning and prioritization of health infrastructure needs to effectively adapt to global warming and cope with future population growth. The approach to assessing future avoidable heat-related mortality may be readily applicable to other parts of the world to address similar issues.

RESULTS

Current mortality attributed to anthropogenic warming

We used two sets of historical simulations to derive the anthropogenic climate change: one is the ALL (anthropogenic and natural forcings), implying consistency with the real world, and the other is the NAT (natural forcings only), indicating a counterfactual scenario without human activities³⁵. Differences between the ALL and NAT can be considered as human-induced outputs, in agreement with previous similar work³⁶. Figure 1 displayed a summary of simulated anthropogenic warming and heat-related mortality. Global mean temperatures simulated by the ALL are significantly higher than the NAT since 1920 (Fig. 1a), meaning that human-induced warming has occurred. During the present day (1995–2014), the human-induced increase in global average temperature has reached around 1.0 °C (95% confidence interval (CI): 0.7–1.2 °C), which is consistent with the report released by the IPCC²⁶. In China, approximately 30% of the national land is now experiencing anthropogenic warming above 1.0 °C, i.e., higher than the worldwide level (Fig. 1b, c). These areas are mostly located in provinces located in parts of Northeast China (NE), Northwest China (NW), North China (NC) and Southwest China (SW), namely at high latitudes and high altitudes in China (Fig. 1c). It is consistent with previous studies indicating that warmings relative to the pre-industrial era (i.e., anthropogenic warming) in these areas are higher than the global level^{27,37–39}. While in Central China (CC), East China (EC) and South China (SC), the human-induced warming are below the global average, which is lower than 0.7 °C.

Based on the historical temperature–mortality relationships archived through the two-stage analysis (Supplementary Fig. 1) and the corresponding location-specific daily temperatures during 1995–2014, the current heat-related mortality is estimated for China and its subregions (Fig. 1d). The outcomes reported higher annual heat-related mortality for the ALL simulations than for the NAT (Supplementary Table 1), indicating that the human activities have caused more thermal deaths. For example, the ALL simulated annual heat-related mortality of 0.017‰ (95% CI: 0.012–0.022‰) in China, compared with 0.015‰ (95% CI: 0.010–0.019‰) simulated by the NAT, with ALL being higher than the NAT. Figure 1e shows the proportion of heat-related deaths caused by human-induced climate change, which can be seen as the anthropogenic impacts on heat risks. Overall for China, human-induced heat-related mortality currently accounts for 17% (95% CI: 13–21%) of total heat mortality, suggesting that natural climate change still dominates heat risk at present. Among the selected subregions, anthropogenic impacts will be greater at high latitudes and altitudes than in other areas, which is similar to the human-induced warming spatial patterns (Fig. 1b). NW currently has the greatest anthropogenic impact (43%, 95% CI: 37–49%), but is still below 50%, and the lowest is in EC (16%, 95% CI: 12–19%). As anthropogenic emissions and climate warming continue in the future, the human-induced impacts on heat-related risks would probably increase.

Overall, more human-induced warming as well as consequent heat-related mortality are currently observed at high latitudes and high altitudes than in other subregions of China. For China and its subregion, natural climate change remains the primary cause of most heat-related deaths today, with anthropogenic influences accounting for less than fifty percent.

Projecting future heat-related mortality based on various scenarios

By the end of this century, the annual mean temperatures projected by the NAT for China and its subregions will remain similar to the baseline (Supplementary Fig. 3), suggesting that global warming would not continue for the long run if anthropogenic emissions stopped immediately. As anthropogenic emissions continue, each future scenario shows increased warming relative to the NAT (Supplementary Fig. 4). Generally speaking, increasing temperatures could imply more extreme heat events, leading to potential rises in heat-related mortality. Especially under the high-emission scenarios (SSP3–7.0 and SSP5–8.5), human-induced warming will increase continuously, whereas it will stop after 2060 under medium- and low-emission scenarios (SSP2–4.5 and SSP1–2.6). Spatially, the high latitudes and high altitudes will continue to experience more human-induced warming than other areas in the future. For example, human-induced temperature increases in NE, NW, NC and SW will reach 7.4–8.3 °C (95% CI: 5.6–9.8 °C) by 2100 under SSP5–8.5, whereas it will be 5.4–6.4 °C (95% CI: 4.3–7.6 °C) in the other subregions. Besides, temporal and spatial changes in population also play an essential role in the amount of heat-related deaths. The projected future populations for China and most subregions show an increasing trend in the short term and will decline thereafter, excluding NE and SW, where the population will keep decreasing in the 21st century. Furthermore, SSP3 will produce a higher population than the other scenarios, with the lowest in SSP5 and SSP1.

For a detailed investigation, we split 2021–2100 into four periods with a 20-year interval, namely 2021–2040, 2041–2060, 2061–2080 and 2081–2100. Assuming a consistent temperature–mortality relationship between the present and the future, the heat-related mortality in 2021–2100 could be estimated by combining the CMIP6 projected daily surface air temperature and the current exposure–response relationship. Figure 2 displays the projected heat-related mortality for China and its subregions based on various scenarios. Under full emission scenarios (i.e., with anthropogenic climate change), China's potential thermal mortality will reach approximately 1.5 times the current level in the next 20 years (2021–2040, 0.027–0.032‰, 95% CI: 0.021–0.039‰), and may quadruple by the end of this century (2081–2100, 0.105‰ under SSP5–8.5, 95% CI: 0.085–0.125‰). Throughout China, the southern areas (EC, SC and SW) will have greater future heat-related mortality than other subregions, with EC and SC being the greatest as well as NC and NE being the lowest. From the comparison between emission scenarios, the differences are less during 2021–2040, while after that the gap between high- and low-emission scenarios increases gradually over time. Especially under SSP5–8.5, future heat-related mortality will be much higher than under other scenarios in 2041–2100. Future high heat-related mortality will cause multiple negative impacts if emissions are not limited^{40,41}.

Anthropogenic warming will increase as emissions rise and over time in the future, with high latitudes and high altitudes continuing to face more warming than other subregions. Combining increased warming with population changes, China's future heat-related mortality will grow significantly, especially in densely populated EC and SC.

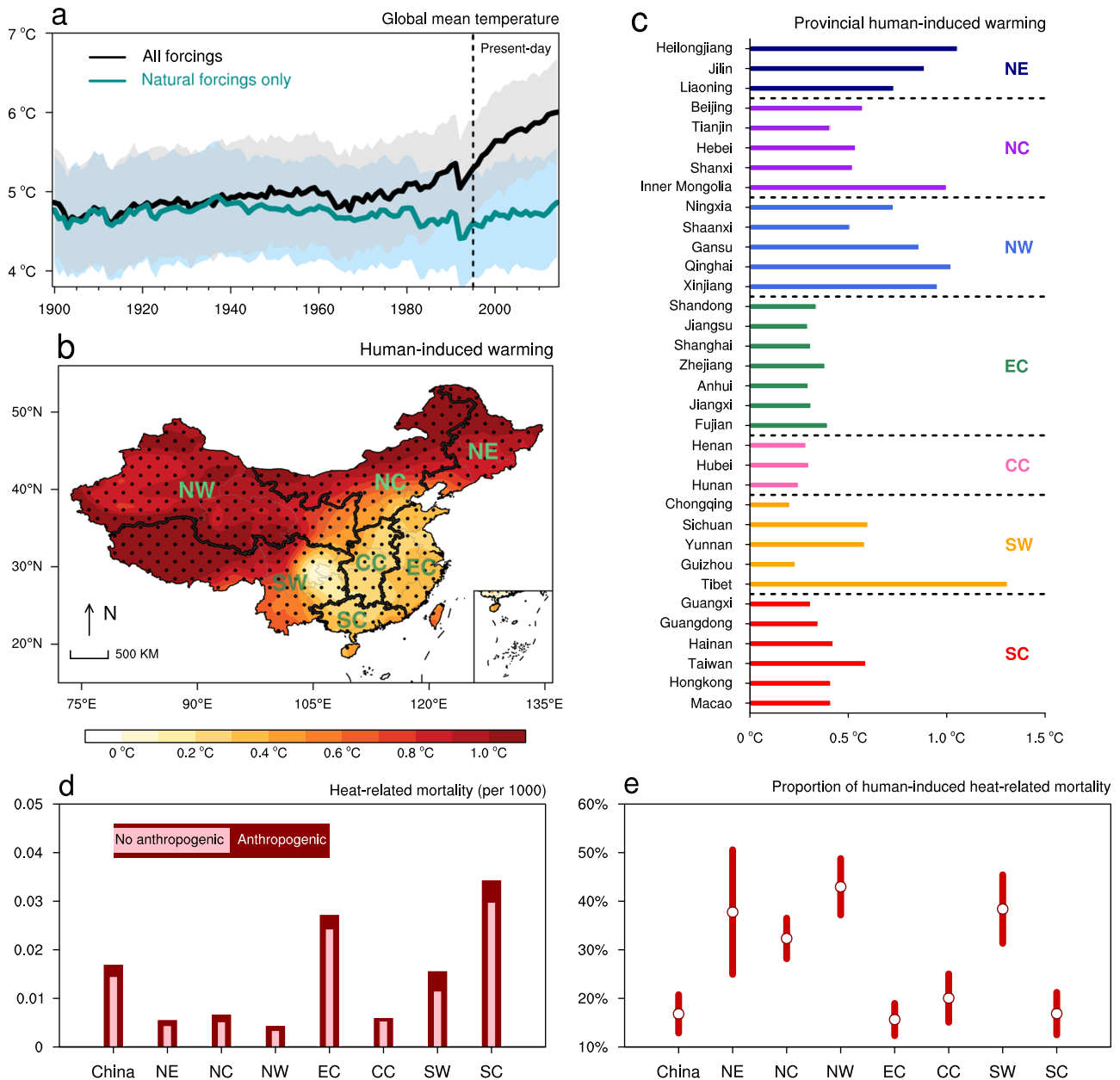


Fig. 1 Human-induced impacts on heat-related mortality in China for the present day (1995–2014). **a** Annual global surface mean temperature from 1900 to 2014, where the solid lines and shaded areas represent multi-model ensemble mean and the model spreads with 95% CI. **b** Spatial patterns of human-induced warming in China for the present day (1995–2014), where dotted areas indicate statistical significance at the 0.05 level according to the *t*-test, and the thick black lines in the maps highlight the subregions. **c** Regional mean human-induced warming for each province in China for the present day. **d** Current annual heat-related mortality (units: ‰), where the dark and light bars indicate the outcomes for ALL (anthropogenic and natural forcings) and NAT (natural forcing only). **e** The proportions of current heat-related deaths attributable to human-induced climate change, with white circles representing the multi-model ensemble mean and lines being model spreads with 95% CI. NE, NC, NW, EC, CC, SW and SC represent Northeast China, North China, Northwest China, East China, Central China, Southwest China and South China, respectively.

Temperature and population change contributions to future heat death

Future projections show that the high-emission scenarios will cause more heat-related deaths in China than the medium- and low-emissions (Fig. 3). EC and SC will have more residents dying from heat events than other subregions due to their high heat-related mortality (Fig. 2) and large population size (Supplementary Fig. 4). On average over 2021–2100, EC and SC will face at least 10,000 heat-related deaths per year, especially under SSP3–7.0 and SSP5–8.5. NW and NE will have the lowest annual heat deaths (500–2000). Given the future

changing ratios relative to the present (Fig. 3b), China's annual heat-related deaths will be about 1.7–3 times the current level. Among the subregions, the future growth rate of heat-related deaths in NW and SC will reach about 2–4 fold, higher than in other regions. Interestingly, the increase in heat-related deaths in all scenarios or subregions over the next 20 years is around 170% of current levels (Supplementary Fig. 5). By 2041–2060, heat-related deaths will begin to rise steadily in the high-emission scenario, but the numbers will peak in the medium-emission and low-emission and begin to decline thereafter. The above implies that the mitigation efforts will hardly

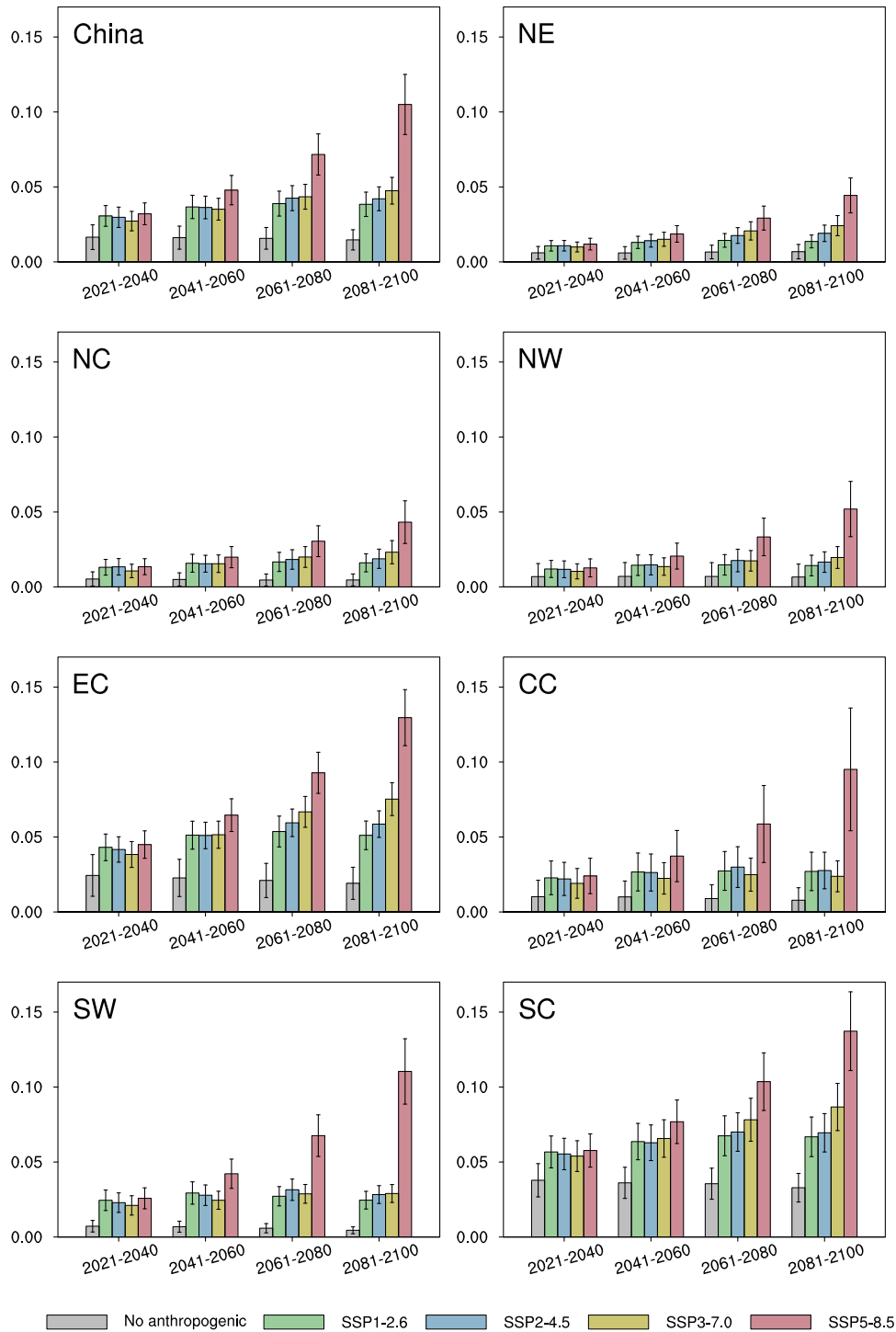


Fig. 2 Projected heat-related mortality for China and seven subregions. Gray, green, blue, yellow, and red bars indicate outcomes for NAT, SSP1–2.6, SSP2–4.5, SSP3–7.0, and SSP5–8.5, respectively (units: %). The vertical black line across the top of each bar depicts the model spreads with 95% CI.

produce immediate effects on heat-related deaths in the near term, and are expected to show up after ~20 years gradually.

From the above findings, it was found that although China's high latitudes and high altitudes would still experience higher anthropogenic warming in the future, due to their sparse population, the number of heat deaths would be much lower than in the densely populated subregions. This suggests that both temperature and population changes have important impacts on heat-related deaths. Here, we quantified the independent contribution of temperature

increase and population change to heat-related deaths in the real world (under ALL simulations) for each future period under different scenarios (Fig. 4). Overall for China, temperature increases and population changes will contribute to about 78 and 22% of heat-related deaths. The contributions of these two factors will be relatively stable in the future, with slight variations in some subregions (e.g., EC and NE). For NW, NE, NC and SW, the contributions of future temperature (population) changes in heat-related deaths are estimated to be 75–95% (5–25%). Compared to these high latitudes

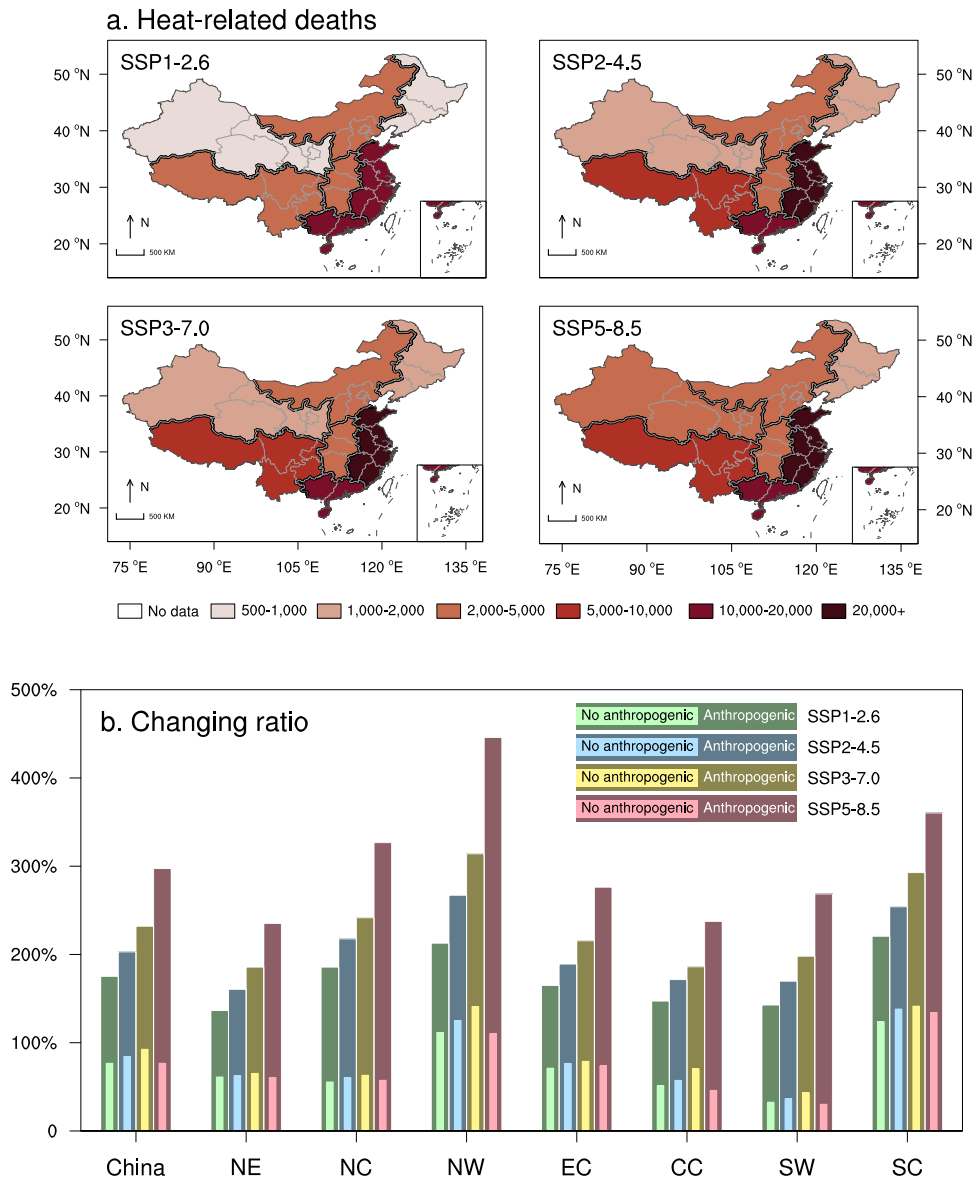


Fig. 3 Projected future heat-related deaths. **a** Future annual heat deaths averaged over 2021–2100 across China for each scenario, where the thick black lines highlight the subregions. **b** Changing ratios of future heat deaths versus the current level. Green, blue, yellow, and red bars respectively indicate outcomes averaged over 2021–2100 for SSP1–2.6, SSP2–4.5, SSP3–7.0, and SSP5–8.5, where the dark (light) bars represent the outcomes of ALL (NAT).

and high altitudes areas, the gap between the contributions of population and temperature changes is narrower in the EC, with the number attributed to temperature (population) ranging between 50 and 75% (25 to 50%). Whereas in CC and SC, population change will dominate heat-related deaths with a contribution of ~55%, about 10% higher than temperature.

In summary, temperature increases at high latitudes and altitudes will strongly dominate heat-related deaths, while population changes will exert a greater impact than the temperature in other regions. Consequently, reducing anthropogenic emissions would be highly beneficial at high latitudes and altitudes, and in other areas, heat risks could also be mitigated by non-climatic factors, such as adjusting demographic distribution and building healthcare infrastructure.

Future potential effects of human-induced warming

The results above show that future heat-related mortality/deaths will increase across China under scenarios with anthropogenic

emissions and that mitigating warming is one of the most effective measures to reduce heat risks. Hence, it is important to quantify the potential future heat-related mortality attributed to human activities, which could inform the maximum heat impacts on public health that might be avoided by reducing emissions. The NAT projections (gray bars in Fig. 2) suggest that China's future heat-related mortality would stay low without anthropogenic emissions, at around 0.015–0.017‰ (95% CI: 0.008–0.025‰), keeping the annual number of heat-related deaths similar to current levels. Except for NW and SC, where heat-related deaths are projected to be 1–1.5 fold of current levels under the NAT (Fig. 3b and Supplementary Fig. 5). Future human-induced heat-related mortality across China will increase more significantly with time and emissions. Each future emission scenario will produce similar anthropogenic heat-related mortality before 2021–2040, after which the high-emission scenario will deliver higher heat-related mortality than the other scenarios (Fig. 5). For example, China's anthropogenic heat-related mortality

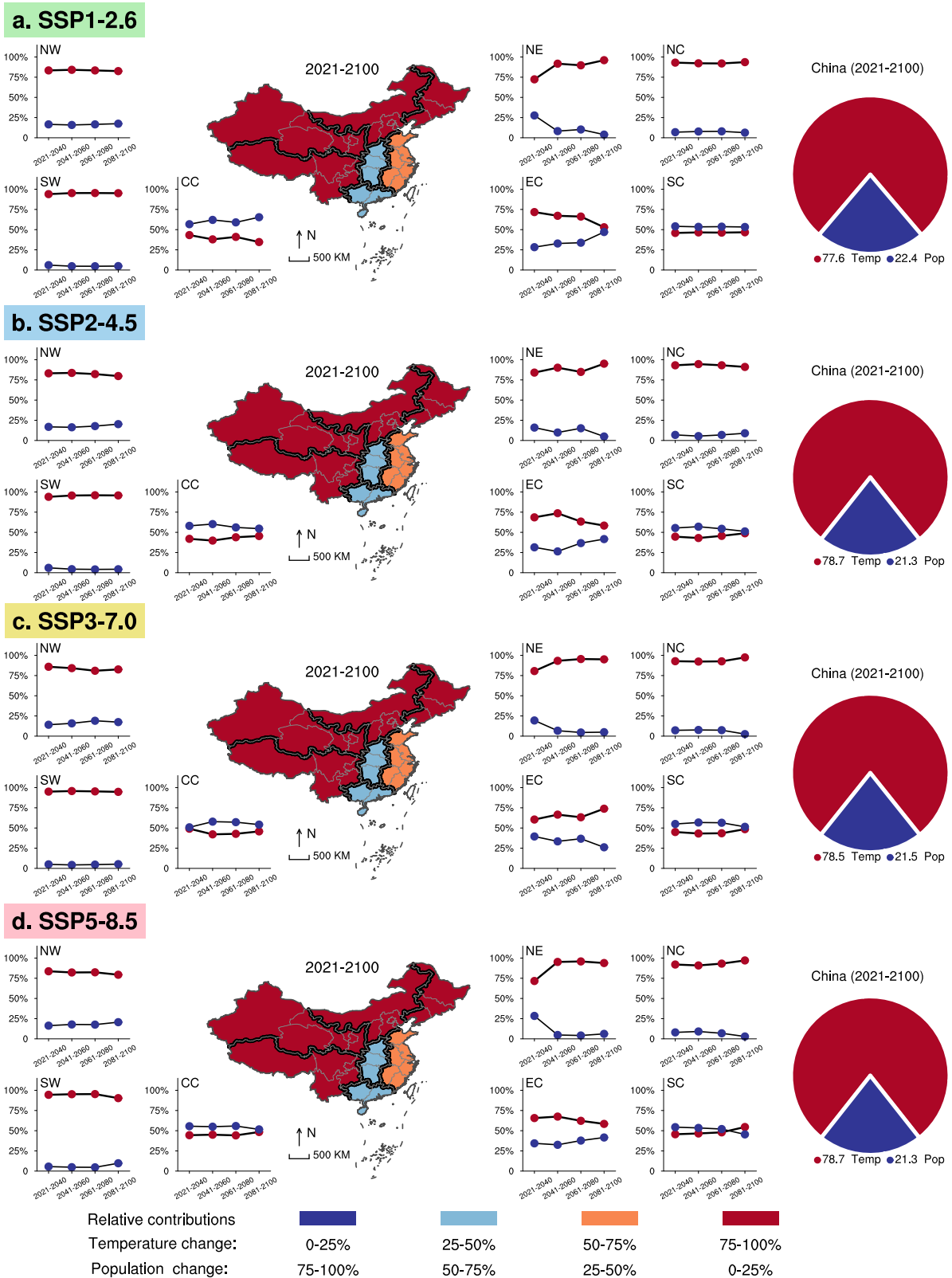


Fig. 4 Future independent contributions of temperature and population changes to heat-related deaths. a–d respectively denotes the results under SSP1–2.6, SSP2–4.5, SSP3–7.0, and SSP5–8.5. Line graphs display contributions of the population (blue) and temperature (red) changes for each region during 2021–2100 at a 20-year interval. Maps highlighting subregions with thick black lines display the major contributions to the heat-related deaths across China averaged over 2021–2100, where red (blue) shaded areas represent temperature (population) as the dominant, with darker colors making greater contributions. Pie charts give the averaged 2021–2100 contributions of the population (blue) and temperature (red) changes to heat-related deaths overall for China.

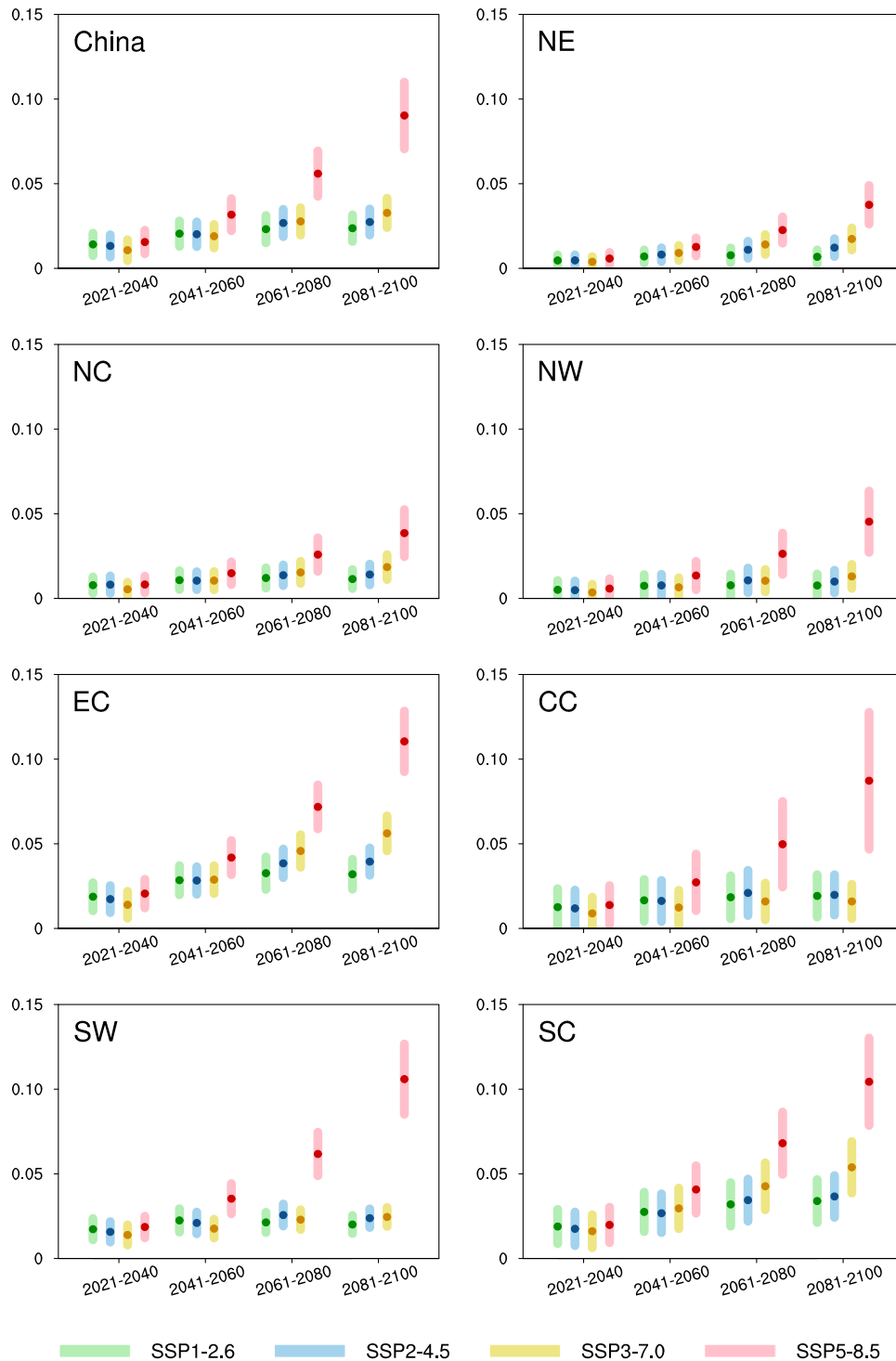


Fig. 5 Projected heat-related mortality associated with human-induced climate change in China and seven subregions. Green, blue, yellow, and red dots (lines) indicate the outcomes (model spreads with 95% CI) averaged for every 20-year interval over 2021–2100 under SSP1–2.6, SSP2–4.5, SSP3–7.0, and SSP5–8.5, respectively (units: ‰).

in 2021–2040 is projected to be around 0.011–0.016‰ (95% CI: 0.005–0.023‰), while under SSP5–8.5 it will increase to 0.090‰ (95% CI: 0.071–0.110‰) in 2081–2100, about threefold higher than under other scenarios. Among the subregions, the human-induced heat-related mortality in EC, SC and SW will be higher than in other subregions.

Regarding the number of future human-induced heat deaths (Supplementary Fig. 6), increases will persist under high-emission

scenarios, while decreases will follow after 2041–2060 under medium- and low-emission scenarios (probably owing to population decline). Over the coming 20 years, anthropogenic warming will cause about 15,576–21,532 (95% CI: 6605–31,183) deaths annually, climbing to 23,139–87,612 (95% CI: 15,470–106,736) by the end of this century. Among the subregions, future heat-related deaths are projected to be fewer in northern China (NE, NC and NW) than in the southern part (EC, SW, and SC), with the least

number in NE (less than 1400 per year). EC will top the subregions in anthropogenic heat-related deaths, accounting for ~40% of the national total, with 5912–8500 (95% CI: 2543–11,985) per year in 2021–2040 and 9265–34,708 (95% CI: 6703–40,332) in 2081–2100. However, the proportion of human-induced heat mortality versus the total count demonstrates a reversed pattern (Supplementary Fig. 7). NW, NE and SW present higher outcomes (above 50%) compared to the other subregions, suggesting that anthropogenic warming is the major responsible for heat-related mortality in these areas. In contrast, the anthropogenic impact is weak in SC, where only 30–50% of future heat-related deaths can be avoided by reducing anthropogenic emissions.

Averaged over 2021–2100, human-induced warming will pose a significant influence on heat health risks in China, accounting for 48–72% (95% CI: 40–76%) of total heat-related mortality (Supplementary Fig. 8), about 2.5–4.0 times worse than today (~17%, Fig. 1e). Also according to the results above (Fig. 3b), China's future heat-related deaths would be slightly lower than present without anthropogenic emissions and would be 1.7–3 fold with anthropogenic emissions. It could be inferred that future potential heat-related deaths without anthropogenic emissions would be 40–70% less than those with anthropogenic emissions. Then by insisting on reducing emissions over the next few decades, there exist possibilities to avoid 40–70% of China's potential heat-related risks, benefiting tens of thousands of people each year. The impacts of anthropogenic warming on human health will also increase with time (Supplementary Fig. 8). From 2021–2040 to 2081–2100, the proportion of heat-related deaths attributed to human activity will increase from 23–37% (95% CI: 8–49%) to 55–86% (95% CI: 47–88%). Especially under SSP5–8.5, these values will grow from 37% (95% CI: 25–49%) in 2021–2040 to 86% (95% CI: 84–88%) in 2081–2100. This suggests that the positive effects of climate change mitigation on public health will be long-term, with benefits increasing over the decades. While in the short term, strategic planning and prioritizing healthcare infrastructure are still needed to effectively adapt to future population changes and climate warming in different regions.

DISCUSSION

Apart from causing climate change, human-induced emissions can also accelerate social and economic development, and with this comes a discussion about whether these advances can mitigate some heat-related health risks. Here, we explore this topic based on historical records from the China Bureau of Statistics, using hospital beds per thousand people and GDP per capita to represent healthcare and economy, respectively. From 1949 to 2020, China experienced rapid economic/medical growth with a significant decline in mortality (Supplementary Fig. 9a). The historical mortality exhibits significant negative correlations with GDP and hospital beds, suggesting that economic growth and healthcare advances have contributed to lower deaths. Then, without the economic and medical development coming with emissions, what would China's heat deaths be like?

We assume that there were no human-induced emissions before, thus leaving China's economy and healthcare at low levels, represented here by the period before the reform and opening (1949–1977, namely P1). Considering that China experienced severe natural disasters from 1959 to 1961⁴², the mortality for this period (around 1-year extension, i.e., 1958–1962) was not counted. The mortality of P1 was 10.75‰, about 1.6 times the baseline period (1995–2014). To obtain heat-related mortality under low-level economic and healthcare development, the baseline temperature simulated by NAT and the P1 mortality was applied. As shown in Supplementary Fig. 9b, without advancements brought by carbon emissions, China's heat mortality would stand 57% above the current level, especially in SC, where the increase would reach 96%. These data suggest that if no previous carbon

emissions were released, although China's warming would be greatly mitigated, the loss of economic and medical advances would also pose more heat-related risks to public health today than in reality. In the future, China's economy will grow rapidly under each emission scenario (suggesting significant improvements in healthcare), especially under SSP5, where GDP per capita will reach eighty times the current level by 2100 (Supplementary Fig. 9c). This probably offset some negative impacts of warming caused by anthropogenic emissions. Therefore, if the mitigation of heat risk by emission-induced economic/medical development is taken into account, the overall findings from this study may overestimate the avoidable future heat-related deaths in China.

Carbon neutrality is being advanced worldwide, and China has declared to achieve this goal by 2060. As more and more countries move towards carbon neutrality, we will probably live in a world with no higher than medium emissions (e.g., SSP1–2.6 and SSP2–4.5) around the mid-century. However, given the inert feature of greenhouse gases in the environment, changes in carbon emission will not have an immediate impact on climate over the next two decades, with significant influences beginning after 2041–2060 (Supplementary Fig. 5). Residents in China will remain at significant thermal risk for the next 20 years. Even if following the low-emission pathway (SSP1–2.6), heat-related deaths in 2021–2040 are still going to reach 1.5–2.0 times higher than today, making emergency responses and medical services facing enormous challenges. Particularly for NW and SC, where the future heat risks from nature climate change will be more severe than the current level. Consequently, alongside insisting on the mitigation of emissions, local urgent emergency response strategies need to be established to manage extreme heat impacts on human health.

There are several limitations to this study. In very hot and humid conditions, the human body's ability to evaporate heat through sweat will decrease, causing heat stress⁴³. This work, like most previous studies^{9,22,23}, has included the effects of humidity and temperature in establishing the DLNM, but only used temperature as the predictor for future investigations. It has been suggested that there will be different changes in relative humidity across China under various future scenarios¹¹. Hence, the humidity will also need to be considered in future predictions of heat-related mortality, but this will involve re-establishing the exposure-response relationships. Furthermore, other meteorological factors (e.g., pollutants, wind speed, sunlight, etc.) may impact the exposure-response relationship between temperature and mortality. Therefore, controlling only humidity in building the DLNM model in this study is also a limitation, and more factors need to be considered in future research. Another shortcoming is that although the population datasets used in this study considered the two-child policy, there may remain discrepancies with the actual future population change in China. Meanwhile, these population datasets do not contain information on age. Considering that different age groups have unequal tolerance for hot weather and that the age structure of China's future population may differ from the current, causing more uncertainty in the estimations. Besides, socioeconomic development will have a potential impact on human adaptation to hot weather. Advances in economic, medical and educational levels will also affect baseline mortality, which would in turn change heat-related mortality^{32,44–49}. We have not yet investigated these issues in depth, which is also the shortcomings of this study.

Uncertainty is also a limitation. In this study, the uncertainties in projecting future heat-related mortality stemmed mainly from differences in temperature–mortality relationships and various CMIP6 simulations. This study employs the multi-model ensemble mean to represent the outcomes with the 95% confidence interval of all simulations as the uncertainties. This is similar to many previous climate projection studies^{10,27,50,51}. Some studies also used the median as the representation of multiple models, which

will not have a large influence on the final results^{23,39}. However, other factors (e.g., human adaptations and technological developments) can also be a source of uncertainty. We assume that future populations would continue to have a similar baseline mortality and temperature–mortality relationship as the current population. Nevertheless, in general, the temperature–mortality relationship will change as the human adaptation to high temperatures changes^{52,53}. For example, the minimum mortality temperature will increase as human tolerance to high temperatures increases^{54,55}. All of the above could contribute to the uncertainties of the risk assessment in this study to some extent. Future assessment work may more accurately predict temperature-related deaths by adjusting exposure–response relationships and baseline mortality with more advanced information. In addition, the construction and development of comprehensive coupled climate–health–economy models can also help project future risks more effectively and provide detailed scientific references for strategic planning^{44,45}.

The findings of independent contributions from temperature and population change to future heat deaths in this study reveal that heat deaths at high latitudes and high altitudes in China are largely dominated by temperature (Fig. 4). These areas, such as NW, SW, NE and NC, are sparsely populated compared to areas like EC, SC and CC. Also, a large number of studies pointed out that these subregions had a sensitive response to global warming, that is, their future temperature increases relative to the current would be higher than those in the rest of China^{27,37–39}. This then raises an interesting question as to whether the heat-related deaths of these regions dominated by temperature changes are due to population sparsity or greater warming or both. Conversely, future population changes in SC and CC contribute more to heat-related deaths than temperature changes, and what could be the reasons for this? All of these issues need to be addressed in depth to provide as detailed information as possible for strategic planning. Furthermore, although the population dataset used in this study has been made considering China's "two-child" policy, there may still be discrepancies from the real situation. Whether this will affect the conclusions of the independent contribution analysis and other sections in this study remains to be examined.

In conclusion, our findings suggest that current heat-related mortality in China is primarily caused by natural climate change, whereas future anthropogenic heat-related mortality will increase by scenario and year, becoming dominant in the next 20–40 years. In comparison with previous studies that mainly focused on projections of future heat risks^{10,19,22,23}, this study specifically demonstrates that cutting human-induced emissions could help prevent 48–72% (95% CI: 40–76%) of future heat-related mortality in China. This is particularly important for high latitudes and altitudes that are highly sensitive to human-induced warming (NW, NE, NC and SW). We also point out that future heat-related deaths will be driven mainly by temperature in most regions, except in CC and SC where population changes will dominate. Notably, as global warming has been long-lasting and has caused some short-term irreversibility^{2,3}, it is unlikely that reducing emissions will bring immediate benefits to mitigate thermal risks in the next two decades. Hence, in addition to insisting on emission reductions, governments and societies have an urgent need to establish sufficient emergency infrastructure and response plans for the potential upcoming increased heat risks^{20,21}.

METHODS

Mortality records

We obtained the daily counts of non-accidental mortality from the Chinese Center for Disease Control and Prevention. According to the International Classification of Diseases-10th Revision (ICD-10),

non-accidental deaths (coded as A00–R99) resulted from diseases rather than from injuries (traffic-related mortalities, suicide, drowning, and so on). A total of 195 fatality surveillance sites distributed across fourteen provinces and three municipalities, covering most of the climate zones in China, were used here (Supplementary Table 2). The mortality records for most locations cover 2010–2016, except Guangzhou and Xining, which are from 2012 to 2016.

Population datasets

The population comes with four shared socioeconomic pathways (SSP1, SSP2, SSP3, and SSP5). They were built on the sixth population census of China in 2010, combining corresponding parameters such as fertility, mortality, migration, and education levels under different SSPs, especially considering China's demographic situation with the comprehensive "two-children" policy^{56–58}. Each SSP includes annual projections from 2010 to 2100 at a latitude–longitude grid spacing of 0.5°. The SSP1 represents sustainable development, meaning less dependence on resources and fossil fuels; SSP2 represents business-as-usual, maintaining the trends of recent decades, achieving some of the development goals, and gradually reducing dependence on fossil fuels; SSP3 represents global, regional rivalry, having large regional disparities, large wealth gaps, unattainable development goals and increased reliance on fossil fuels; SSP5 stands for fossil-fueled development, with economic development focused on mitigating challenges and solving socioeconomic problems through the pursuit of self-interest¹³.

Climate model simulations and projections

Based on the daily mean surface air temperature availability we used eleven models in the CMIP6 archives. These climate models came from nine countries around the world, and only the first realization of each model was selected for the analysis (Supplementary Table 3). They comprise a set of historical simulations (1900–2014) and future projections (2021–2100), with the ALL (anthropogenic and natural forcings) and NAT (natural forcings only) outputs. The historical ALL shows the real world and the future ones include the outcomes under four designed emission scenarios (SSP1–2.6, SSP2–4.5, SSP3–7.0, and SSP5–8.5), while the NAT represents a counterfactual situation. Similar to previous studies^{7,18,36,59}, differences between the ALL and NAT simulates indicate human-induced climate impacts which represents the cap on the avoidable abatement benefits. Besides, dividing the anthropogenic outcomes (ALL minus NAT) by the ALL simulations gives the proportion of human-induced impacts. For example, the proportion of heat-related mortality attributable to anthropogenic effects is the human-induced heat-related mortality divided by the overall heat-related mortality (Fig. 1e).

SSP5–8.5, SSP3–7.0, SSP2–4.5, and SSP1–2.6 indicate carbon emissions from high to low. SSP5–8.5 is the only SSP scenario with high enough emission (SSP5) to generate a radiative forcing of $8.5 \text{ W} \cdot \text{m}^{-2}$ in 2100. SSP3–7.0 combines relatively high societal vulnerability (SSP3) with a relatively high forcing of $7.0 \text{ W} \cdot \text{m}^{-2}$. SSP2–4.5 combines intermediate societal vulnerability (SSP2) with an intermediate forcing of $4.5 \text{ W} \cdot \text{m}^{-2}$. SSP1–2.6 combines low vulnerability with low challenges for mitigation (SSP1) as well as a low forcing of $2.6 \text{ W} \cdot \text{m}^{-2}$. We applied adjusted the resolutions of the climate data by bilinear interpolation to $0.5^\circ \times 0.5^\circ$, corresponding to the population datasets.

Economic and medical level relevant information

Gross domestic product (GDP) and hospital bed records from the China Statistical Yearbook for 1949–2021 were used to respectively denote the historical Chinese economy and healthcare levels, and the 2022–2100 gridded GDP projections provided by

Jiang et al.⁵⁷ were used to represent future potential economic development. We used these datasets to discuss the possible relationship between economic development from emissions and changes in heat-related mortality.

Study regions and periods

Seven subregions are highlighted according to the geographic zoning of China¹⁰ (Fig. 1b, c), which are Northeast China (NE), North China (NC), Northwest China (NW), East China (EC), Central China (CC), Southwest China (SW), and South China (SC). We selected the present-day period of 1995–2014 as the baseline and 2021–2100 as the future period, consistent with previous studies^{11,27}.

Historical temperature–mortality relationship

A two-stage analysis based on 195 sites across China was used to estimate the historical association between temperature and mortality.

In the first stage, a quasi-Poisson regression with a distributed lag non-linear model (DLNM) was built to fit the temperature–mortality relationship at each location by using daily observed temperature and mortality records⁶⁰. We introduced a cross-basis function in DLNM to model the non-linear and lagged impacts of temperature on mortality. The “crosspred” function, which is used to predict the DLNM, is introduced and the reference predicted values are computed. The DLNM is as follows:

$$\text{Log}[E(Y_i)] = a + \beta T_{i,l} + ns(\text{time}, df) + ns(\text{rh}, df) + DOW \quad (1)$$

where Y_i denotes the observed daily mortality at calendar day i , a is the intercept, $T_{i,l}$ represents the cross-basis matrix for the bi-dimensions of the temperature (T) and lag days, β denotes the vector of coefficients for $T_{i,l}$, and ns is the natural cubic spline function. In addition, DOW is the effect of the day of the week, and df represents the degree of freedom (df). Based on previous studies, a natural cubic spline with 3 df was used to adjust for the effect of relative humidity (rh) and a natural cubic spline with 7 df per year was used for time to control for long-term temporal trends. We selected a lag period of 21 days (Supplementary Fig. 2), which is sufficient to capture the lagging effects of temperature and would not lead to over-fitting²³. More details on analytical methods and the modeling process can be found in previous studies^{9,23,61}.

Given the differences in health impacts between urban and rural areas, the temperature–mortality relationship in different provinces (autonomous regions) cannot simply be assessed within the provincial capitals, but heat-related health risks are similar in the same climate zone^{62,63}. A multivariate meta-analysis based on the restricted maximum likelihood was performed in the second stage to examine the pooled temperature–mortality relationship and to show the regional patterns of mortality risks related to temperature. Then, the best linear unbiased prediction (BLUP) was used to predict the cumulative temperature–mortality relationship for each region. Details of this methodology have been described in the previous study⁶⁴. Finally, the heterogeneity was tested by Cochran’s Q method and extension of the I^2 statistic.

The above methods are commonly used and widely accepted for analyzing the temperature–mortality relationship, which can be performed by combining all points in a region and thus obtaining a temperature–mortality exposure-response curve that is representative of the region^{9,23,65–68}.

Estimated heat-related mortality and deaths

Similar to previous studies^{9,23,66,67}, this study estimated temperature–mortality relationships and the heat-related mortality from non-accidental causes; and gained CMIP6 multi-model outputs. For each grid point, we first calculated the daily

temperature-related deaths and then obtained the annual heat-related deaths by summing the days with temperatures above the minimum mortality temperature (MMT, which has an RR of 1). Furthermore, heat-related mortality was obtained by dividing the heat-related deaths by the corresponding gridded population. Notably, the regional heat-related deaths are the sum of the heat deaths at each grid point within the region and the regional heat-related mortality is the regional deaths divided by the regional population. The calculation is as follows:

$$AF = \frac{RR - 1}{RR} \quad (2)$$

$$AD_{x,d} = Mort_{x,y} \times Pop_{x,y} \times AF_{x,d} \quad (3)$$

$$HD_{x,y} = \sum \{AD_{x,d}\} \dots \dots (\text{When } T_{x,d} > MMT) \quad (4)$$

$$HM_{x,y} = \frac{HD_{x,y}}{Pop_{x,y}} \quad (5)$$

$$\text{Regional_}HD_y = \sum \{HD_{x,y}\} \quad (6)$$

$$\text{Regional_}HM_y = \frac{\text{Regional_}HD_y}{\sum \{Pop_{x,y}\}} \quad (7)$$

where AF is the attribute fraction (AF) of the specific temperature, computed from the relative risks (RR) by the DLNM and meta-analysis in different subregions, and the exposure-response relationship is assumed to be consistent during the study periods. $Pop_{x,y}$ and $Mort_{x,y}$ refer to the population and baseline mortality at grid x in year y . $AD_{x,d}$ and $T_{x,d}$ are the daily temperature-related deaths and the model simulated daily mean temperature for day d in year y . $HD_{x,y}$ and $HM_{x,y}$ represent the annual heat-related deaths and mortality. $\text{Regional_}HD_y$ and $\text{Regional_}HM_y$ represent the regional annual heat-related deaths and mortality. In this study, the MMT for NE, NC, NW, EC, CC, SW, and SC was approximately 22 °C, 25 °C, 24 °C, 25 °C, 26 °C, 26 °C, and 25 °C, respectively (Supplementary Fig. 1).

Uncertainty analysis

Like previous studies^{10,17,69}, uncertainties in projections of future heat-related mortality in this study arise mainly from the temperature–mortality relationship and variations in the simulated temperature of different CMIP6 models. Specifically, we quantified these uncertainties by generating 1000 samples of reduced BLUP coefficients using Monte Carlo simulation⁷⁰, with the assumption that the estimates follow a multivariate normal distribution, and then producing results for each selected CMIP6 model^{69,71}. We used the multi-model ensemble mean to represent the overall CMIP6 outputs^{11,16}, with a 95% confidence interval (CI) as the uncertainty. The 95% CI was defined as the 2.5th and 97.5th percentiles of the empirical distribution across the CMIP6 model results.

Independent contributions of temperature and population changes

To detail the impacts of temperature and population changes on heat-related mortality across scenarios/periods/regions, we applied the Gini importance computed from Random Forest⁷² to figure out the independent contributions of the inner factors. The random forest structure can be thought of as a set of decision trees, each containing internal nodes and leaves. In the internal nodes, the selected features are used to decide how to partition the dataset into two independent sets with similar internal responses. The features of the internal nodes are selected with some criteria, which for classification jobs can be Gini impurity or information gain, and for regression, variance reduction. We can

measure how each feature reduces the split impurity (the feature with the most reduction is selected as the internal node). For each feature, we can collect how on average it reduces impurity. The average for all trees in the forest is what measures the importance of the feature.

Here, we quantified the independent contributions of temperature and population changes to heat-related mortality in each subregion across different periods/scenarios. Based on the multi-model results, for each grid point with inhabitants in the subregion, we included the corresponding population, annual mean heat-related daily temperature (i.e., the average temperature of the days above the MMT) and annual heat-related deaths in the Random Forest model for simulation. The Gini importance of temperature and population from the Random Forest output was multiplied by 100% to indicate their respective independent contributions.

DATA AVAILABILITY

The dataset generated and analyzed during this study is available (with some institutional limitations) from the corresponding authors upon reasonable request. The mortality data can be obtained from the Chinese Center for Disease Control and Prevention under the agreement to not engage in the unauthorized distribution of the raw data to a third party and to use the data for scientific research only (<http://www.phs-science.com/Share/en/index.jsp>). Historical daily meteorological data are from China Meteorological Data Service Center (<http://data.cma.cn/>). The CMIP6 outputs can be found at <https://esgf-node.llnl.gov/projects/cmip6>. Historical China's GDP and hospital bed records are from the China Statistical Yearbook collected by the National Bureau of Statistics (<http://www.stats.gov.cn/>). Gridded population and GDP projections of China are provided by Professor Jiang Tong's team from the Institute for Disaster Risk Management at Nanjing University of Information Science and Technology.

CODE AVAILABILITY

The above analyses were performed using R (version 4.2), Python (version 3.9), and NCL (version 6.6), and the code is available on request.

Received: 22 November 2022; Accepted: 15 June 2023;

Published online: 08 July 2023

REFERENCES

- Casanueva, A. et al. Climate projections of a multivariate heat stress index: the role of downscaling and bias correction. *Geosci. Model Dev.* **12**, 3419–3438 (2019).
- IPCC. Summary for policymakers. *Climate Change 2021: The Physical Science Basis*. Contribution of Working Group I to the Sixth Assessment Report of the Intergovernmental Panel on Climate Change (eds Masson-Delmotte, V. et al.) (IPCC, 2021).
- IPCC. *Climate Change 2022: Mitigation of Climate Change*. Contribution of Working Group III to the Sixth Assessment Report of the Intergovernmental Panel on Climate Change (eds Shukla, P. R. et al.) (IPCC, 2022).
- Baldwin, J. W., Dessy, J. B., Vecchi, G. A. & Oppenheimer, M. Temporally compound heat wave events and global warming: an emerging hazard. *Earth's Future* **7**, 411–427 (2019).
- Dematte, J. E. et al. Near-fatal heat stroke during the 1995 heat wave in Chicago. *Ann. Intern. Med.* **129**, 173–181 (1998).
- Robine, J. M. et al. Death toll exceeded 70,000 in Europe during the summer of 2003. *C. R. Biol.* **331**, 171–178 (2008).
- Fischer, E. M. & Knutti, R. Anthropogenic contribution to global occurrence of heavy-precipitation and high-temperature extremes. *Nat. Clim. Change* **5**, 560–564 (2015).
- Schiermeier, Q. Climate change made North America's deadly heatwave 150 times more likely. *Nature* <https://doi.org/10.1038/d41586-021-01869-0> (2021).
- Xing, Q. et al. Impacts of urbanization on the temperature-cardiovascular mortality relationship in Beijing, China. *Environ. Res.* **191**, 110234 (2020).
- Yang, J. et al. Projecting heat-related excess mortality under climate change scenarios in China. *Nat. Commun.* **12**, 1039 (2021).
- Zhang, G. W., Zeng, G., Liang, X. Z. & Huang, C. R. Increasing heat risk in China's urban agglomerations. *Environ. Res. Lett.* **16**, 064073 (2021).
- Moss, R. H. et al. The next generation of scenarios for climate change research and assessment. *Nature* **463**, 747–756 (2010).
- O'Neill, B. C. et al. The roads ahead: narratives for shared socioeconomic pathways describing world futures in the 21st century. *Global Environ. Change* **42**, 169–180 (2017).
- Kriegler, E. et al. *Socio-Economic Scenario Development for Climate Change Analysis*. CIRED Working Papers, CIRED, 2010-10-23 (2010).
- Eyring, V. et al. Overview of the Coupled Model Intercomparison Project Phase 6 (CMIP6) experimental design and organization. *Geosci. Model Dev.* **9**, 1937–1958 (2016).
- Iyakaremye, V. et al. Increased high-temperature extremes and associated population exposure in Africa by the mid-21st century. *Sci. Total Environ.* **790**, 148162 (2021).
- Wang, J. et al. Anthropogenic emissions and urbanization increase risk of compound hot extremes in cities. *Nat. Clim. Change* **11**, 1084–1089 (2021).
- Wang, J. et al. Anthropogenically-driven increases in the risks of summertime compound hot extremes. *Nat. Commun.* **11**, 528 (2020).
- Wang, Y. J. et al. Tens of thousands additional deaths annually in cities of China between 1.5 °C and 2.0 °C warming. *Nat. Commun.* **10**, 3376 (2019).
- Cai, W. et al. The 2020 China report of the Lancet Countdown on health and climate change. *Lancet Public Health* **6**, e64–e81 (2021).
- Cai, W. et al. The 2021 China report of the Lancet Countdown on health and climate change: seizing the window of opportunity. *Lancet Public Health* **6**, e932–e947 (2021).
- Sun, Z. et al. Projection of temperature-related excess mortality by integrating population adaptability under changing climate—China, 2050s and 2080s. *China CDC Wkly.* **3**, 697–701 (2021).
- Xing, Q. et al. Projections of future temperature-related cardiovascular mortality under climate change, urbanization and population aging in Beijing, China. *Environ. Int.* **163**, 107231 (2022).
- Huang, C. et al. Projecting future heat-related mortality under climate change scenarios: a systematic review. *Environ. Health Perspect.* **119**, 1681–1690 (2011).
- Guo, Y., Barnett, A. G., Pan, X., Yu, W. & Tong, S. The impact of temperature on mortality in Tianjin, China: a case-crossover design with a distributed lag non-linear model. *Environ. Health Perspect.* **119**, 1719–1725 (2011).
- IPCC. *Global warming of 1.5 °C*. An IPCC Special Report on the impacts of global warming of 1.5 °C above pre-industrial levels and related global greenhouse gas emission pathways, in the context of strengthening the global response to the threat of climate change, sustainable development, and efforts to eradicate poverty (eds Masson-Delmotte, V. et al.) (2018).
- Zhang, G. W., Zeng, G., Yang, X. Y. & Jiang, Z. H. Future changes in extreme high temperature over China at 1.5 °C -5 °C global warming based on CMIP6 simulations. *Adv. Atmos. Sci.* **38**, 253–267 (2021).
- Sun, Q. H., Miao, C. Y., AghaKouchak, A. & Duan, Q. Y. Unraveling anthropogenic influence on the changing risk of heat waves in China. *Geophys. Res. Lett.* **44**, 5078–5085 (2017).
- Jiang, T. et al. National and provincial population projected to 2100 under the shared socioeconomic pathways in China. *Clim. Change Res.* **13**, 128–137 (2017).
- Zander, K. K., Cadag, J. R., Escarcha, J. & Garnett, S. T. Perceived heat stress increases with population density in urban Philippines. *Environ. Res. Lett.* **13**, 084009 (2018).
- Zhao, L. et al. Global multi-model projections of local urban climates. *Nat. Clim. Change* **11**, 152–157 (2021).
- Rai, M. et al. Future temperature-related mortality considering physiological and socioeconomic adaptation: a modelling framework. *Lancet Planet. Health* **6**, e784–e792 (2022).
- He, G. H. et al. The assessment of current mortality burden and future mortality risk attributable to compound hot extremes in China. *Sci. Total Environ.* **777**, 146219 (2021).
- Zhang, X., Guo, F. & Zhai, Z. China's demographic future under the new two-child policy. *Popul. Res. Policy Rev.* **38**, 537–563 (2019).
- Mao, J. F. et al. Human-induced greening of the northern extratropical land surface. *Nat. Clim. Change* **6**, 959–963 (2016).
- Vicedo-Cabrera, A. M. et al. The burden of heat-related mortality attributable to recent human-induced climate change. *Nat. Clim. Change* **11**, 492–500 (2021).
- Li, D., Zhou, T., Zou, L., Zhang, W. & Zhang, L. Extreme high-temperature events over East Asia in 1.5 °C and 2 °C warmer futures: analysis of NCAR CESM low-warming experiments. *Geophys. Res. Lett.* **45**, 1541–1550 (2018).
- Li, D., Zou, L. & Zhou, T. Extreme climate event changes in China in the 1.5 and 2 °C warmer climates: results from statistical and dynamical downscaling. *J. Geophys. Res. Atmos.* **123**, 10,215–10,230 (2018).
- Zhang, G. W., Zeng, G., Iyakaremye, V. & You, Q. L. Regional changes in extreme heat events in China under stabilized 1.5 °C and 2.0 °C global warming. *Adv. Clim. Change Res.* **11**, 198–209 (2020).

40. Ma, M., Cai, W., Cai, W. & Dong, L. Whether carbon intensity in the commercial building sector decouples from economic development in the service industry? Empirical evidence from the top five urban agglomerations in China. *J. Clean. Prod.* **222**, 193–205 (2019).
41. Ma, X., Liu, Z. & Wang, Y. Application of a novel nonlinear multivariate grey Bernoulli model to predict the tourist income of China. *J. Comput. Appl. Math.* **347**, 84–94 (2019).
42. Huang, C., Li, Z., Wang, M. & Martorell, R. Early life exposure to the 1959–1961 Chinese famine has long-term health consequences. *J. Nutr.* **140**, 1874–1878 (2010).
43. Mora, C. et al. Global risk of deadly heat. *Nat. Clim. Change* **7**, 501–506 (2017).
44. Cromar, K., Howard, P., Vasquez, V. N. & Anthoff, D. Health impacts of climate change as contained in economic models estimating the social cost of carbon dioxide. *Geohealth* **5**, e2021GH000405 (2021).
45. Cromar, K. R. et al. Global health impacts for economic models of climate change: a systematic review and meta-analysis. *Ann. Am. Thorac. Soc.* **19**, 1203–1212 (2022).
46. Halpern-Manners, A., Helgert, J., Warren, J. R. & Roberts, E. The effects of education on mortality: evidence from linked U.S. census and administrative mortality data. *Demography* **57**, 1513–1541 (2020).
47. Keefer, C. S. The impact of research and medical education on public health. *Public Health Rep.* **69**, 80–84 (1954).
48. Kernick, D. P. The impact of health economics on healthcare delivery. A primary care perspective. *Pharmacoeconomics* **18**, 311–315 (2000).
49. Lee, J. Y. & Kim, H. Projection of future temperature-related mortality due to climate and demographic changes. *Environ. Int.* **94**, 489–494 (2016).
50. Chen, H. et al. Projections of heatwave-attributable mortality under climate change and future population scenarios in China. *Lancet Reg. Health West. Pac.* **28**, 100582 (2022).
51. Gu, S. et al. Projections of temperature-related cause-specific mortality under climate change scenarios in a coastal city of China. *Environ. Int.* **143**, 105889 (2020).
52. Ilardo, M. & Nielsen, R. Human adaptation to extreme environmental conditions. *Curr. Opin. Genet. Dev.* **53**, 77–82 (2018).
53. Hondula, D. M., Balling, R. C., Vanos, J. K. & Georgescu, M. Rising temperatures, human health, and the role of adaptation. *Curr. Clim. Change Rep.* **1**, 144–154 (2015).
54. Krummenauer, L., Costa, L., Prah, B. F. & Kropp, J. P. Future heat adaptation and exposure among urban populations and why a prospering economy alone won't save us. *Sci. Rep.* **11**, 20309 (2021).
55. Yin, Q., Wang, J. F., Ren, Z. P., Li, J. & Guo, Y. M. Mapping the increased minimum mortality temperatures in the context of global climate change. *Nat. Commun.* **10**, 4640 (2019).
56. Huang, J. L. et al. Effect of fertility policy changes on the population structure and economy of China: from the perspective of the shared socioeconomic pathways. *Earth's Future* **7**, 250–265 (2019).
57. Jiang, T. et al. Gridded datasets for population and economy under shared socioeconomic pathways for 2020–2100. *Clim. Change Res.* **18**, 381–383 (2022).
58. Jing, C. et al. Population, urbanization and economic scenarios over the Belt and Road region under the shared socioeconomic pathways. *J. Geogr. Sci.* **30**, 68–84 (2020).
59. Pei, L., Yan, Z., Chen, D. & Miao, S. The contribution of human-induced atmospheric circulation changes to the record-breaking winter precipitation event over Beijing in February 2020. *BAMS* **103**, S55–S60 (2022).
60. Gasparrini, A., Armstrong, B. & Kenward, M. G. Distributed lag non-linear models. *Stat. Med.* **29**, 2224–2234 (2010).
61. Yang, J. et al. Heatwave and mortality in 31 major Chinese cities: definition, vulnerability and implications. *Sci. Total Environ.* **649**, 695–702 (2019).
62. Chen, R. et al. Association between ambient temperature and mortality risk and burden: time series study in 272 main Chinese cities. *BMJ* **363**, k4306 (2018).
63. Chen, H. et al. Spatiotemporal variation of mortality burden attributable to heatwaves in China, 1979–2020. *Sci. Bull.* **67**, 1340–1344 (2022).
64. Gasparrini, A. et al. Mortality risk attributable to high and low ambient temperature: a multicountry observational study. *Lancet* **386**, 369–375 (2015).
65. Gasparrini, A. & Armstrong, B. Reducing and meta-analysing estimates from distributed lag non-linear models. *BMC Med. Res. Methodol.* **13**, 1 (2013).
66. Huang, C. et al. Mortality burden attributable to heatwaves in Thailand: a systematic assessment incorporating evidence-based lag structure. *Environ. Int.* **121**, 41–50 (2018).
67. Hu, J. et al. Temperature-related mortality in China from specific injury. *Nat. Commun.* **14**, 37 (2023).
68. Huang, C. R., Barnett, A. G., Wang, X. M. & Tong, S. L. The impact of temperature on years of life lost in Brisbane, Australia. *Nat. Clim. Change* **2**, 265–270 (2012).
69. Gasparrini, A. et al. Projections of temperature-related excess mortality under climate change scenarios. *Lancet Planet. Health* **1**, e360–e367 (2017).
70. Bonate, P. L. A brief introduction to Monte Carlo simulation. *Clin. Pharmacokinet.* **40**, 15–22 (2001).
71. Vicedo-Cabrera, A. M., Sera, F. & Gasparrini, A. Hands-on tutorial on a modeling framework for projections of climate change impacts on health. *Epidemiology* **30**, 321–329 (2019).
72. Breiman, L. Random forests. *Mach. Learn.* **45**, 5–32 (2001).

ACKNOWLEDGEMENTS

We thank the reviewers for their constructive comments. This work is supported by the National Natural Science Foundation of China (42205170 and 42175184), the Public health service capability improvement project from the National Health Commission of the People's Republic of China (2100409034), the Project from the National Bureau of Foreign Experts (G2022065004L), the Youth Beijing Scholars Program (2018–007), Key innovation team of China Meteorological Administration (CMA2022ZD09), the Open Grants of the State Key Laboratory of Severe Weather (2023LASW-B19 and 2023LASW-B26), and the Beijing Meteorological Bureau (BMBKJ202201005 and BMBKJ202201007). We thank Professor Jiang Tong's team from the Institute of Disaster Risk Management at Nanjing University of Information Science and Technology for providing detailed population and GDP data.

AUTHOR CONTRIBUTIONS

Conceptualization: G.Z. and Z.S.; methodology: G.Z., L.H., and Z.S.; software: G.Z., L.H., and Z.X.; investigation: G.Z. and Z.S.; data curation: G.Z. and L.H.; writing: G.Z., Z.S., L.H., V.I., and S.T.; supervision: Z.S., S.M., and S.T.; funding acquisition: G.Z., Z.S., and L.H.

COMPETING INTERESTS

The authors declare no competing interests.

ADDITIONAL INFORMATION

Supplementary information The online version contains supplementary material available at <https://doi.org/10.1038/s41612-023-00404-4>.

Correspondence and requests for materials should be addressed to Zhaobin Sun or Shilu Tong.

Reprints and permission information is available at <http://www.nature.com/reprints>

Publisher's note Springer Nature remains neutral with regard to jurisdictional claims in published maps and institutional affiliations.



Open Access This article is licensed under a Creative Commons Attribution 4.0 International License, which permits use, sharing, adaptation, distribution and reproduction in any medium or format, as long as you give appropriate credit to the original author(s) and the source, provide a link to the Creative Commons license, and indicate if changes were made. The images or other third party material in this article are included in the article's Creative Commons license, unless indicated otherwise in a credit line to the material. If material is not included in the article's Creative Commons license and your intended use is not permitted by statutory regulation or exceeds the permitted use, you will need to obtain permission directly from the copyright holder. To view a copy of this license, visit <http://creativecommons.org/licenses/by/4.0/>.

© The Author(s) 2023